The photophysics of solution processable semiconductors for applications in optoelectronic devices

Abdu-Aguye, Mustapha

DOI:
10.33612/diss.111696164

Chapter 2

The effect of PbS nanocrystal additives on the charge transfer state recombination in a bulk heterojunction blend

This chapter describes the use of lead sulphide nanocrystals (PbS QDs) as high dielectric constant (ε_r) additives in a bid to investigate a persistent limitation of organic semiconductors: their low dielectric constant, which limits the performance of bulk heterojunction (BHJ) solar cells. The approach utilizes the recombination of the interfacial charge transfer (CT) state as a means to study the effects of PbS QDs on blends composed of the narrow bandgap copolymer: poly [2,6-(4,4-bis-(2-ethylhexyl)-4H-cyclopenta[2,1-b;3,4-b']dithiophene)-alt-4,7-(2,1,3-benzothiadiazole)] (PCPDTBT), and a fullerene derivative: phenyl-C_{61}-butyric acid methyl ester (PCBM).

This chapter is based on the publication:

M. Abdu-Aguye, L. Protesescu, D. N. Dirin, M. V. Kovalenko, M. A. Loi, *Org. Photonics Photovoltaics* **2018**, 1.

2.1 Introduction

Semiconducting polymers blended with small molecule acceptors in what is commonly called the bulk-heterojunction (BHJ) configuration hold great promise as active layers of solar cells. Large advancements have been obtained in the performance of these devices in the last years, reaching nowadays power conversion efficiencies as high as 11.7%.[1] This is because of progresses in synthetic techniques, film fabrication, interfacial layer optimization and other aspects of device engineering.[2,3]

BHJ solar cells consist of a bicontinuous 3-dimensional network of a so-called *donor* polymer and an acceptor, which is usually a molecule with a high electron affinity. The donor's primary function is to absorb light, forming a Coulombically bound electron-hole pair, and to provide a conduction path for the leftover hole to the anode after the electron transfer has occurred. While the acceptor's function is to assist in exciton dissociation and to provide a pathway for electrons to be transported to the cathode of the device.

The intrinsically low dielectric constant ($2 < \varepsilon_r < 3$) of many semiconducting organic materials results in a strongly bound *Frenkel* exciton;[4] which requires about 0.3-0.5eV to be split into free charges.[5] This energy, the exciton binding energy E_b, is experimentally apparent as a loss in the open circuit voltage V_{oc} of the solar cell.[6] An important intermediate excitation occurring in many BHJs is the *charge transfer* (CT) state. This state has been described as an interfacial charge pair between the donor-acceptor heterointerface, where the electron is spatially localised on an acceptor molecule, and the hole on the donor.[7] Many authors have reported a low energy emission coming from the recombination of these states as well as a sub-bandgap absorption in some BHJs.[8–10] The CT state therefore plays a crucial role in the operation of BHJ solar cells, which is detrimental if it leads to a loss of photogenerated carriers.[11] In order to overcome the coulombic attraction between the electron-hole pair in the CT state, a viable strategy is to increase the dielectric constant of the BHJ.[5] This would help to effectively screen the Coulomb interaction, thus decreasing E_b, and therefore also to influence the CT state recombination rate.[11]

To increase the ε_r of BHJ films, there are two main approaches. The first involves molecular engineering, i.e., synthesizing donor or acceptor molecules with large dipole moments; for example, using highly polarizable units for the polymer[12] or

using highly polar side groups in fullerenes.[13] Another possibility involves the use of high-ε_r additives. Although there have been reports of both donor polymers and fullerenes with increased ε_r[14–18]; the former method has proven to be very challenging for synthetic chemists. Furthermore, though the Debye formulation of the Clausius-Mosotti (CM) equation suggests that molecules with a large dipole moment will have a high ε_r; established models for charge transport in disordered organic semiconductors suggest that (dipolar) disorder in films of highly polar molecules negatively affects charge mobilities and causes a broadening of the DOS;[19,20] implying that simply adding highly polar groups to polymers as a strategy to improve ε_r is unlikely to be a straightforward task. Moreover, very often dipoles can compensate each other in thin films leaving the final dielectric constant unchanged.[21,22]

In this chapter, we report on the use of oleic-acid capped lead sulphide (PbS-OA) nanocrystals, also referred to as Quantum dots (QDs) as a high dielectric constant additive for polymer BHJs. PbS-OA QDs are an interesting additive because in thin films, they exhibit ε_r >20,[23] and can be solution processed from organic solvents compatible with BHJ fabrication. A prototypical BHJ composed of poly[2,6-(4,4-bis-(2-ethylhexyl)-4H-cyclopenta[2,1-b;3,4-b']dithiophene)-alt-4,7-(2,1,3-benzothiadiazole)] hereafter referred to as PCPDTBT and phenyl-C_{61}-butyric acid methyl ester ($PC_{61}BM$) were chosen for the rather strong CT photoluminescence (QY =0.03%),[24] which has been proposed to be dependent on the ε_r of the blend.[25] Thus, with this material combination, the CT photoluminescence can be used as a "fingerprint" to study the effect of the local dielectric constant on the photoexcitations of BHJs. We show that with a little addition of PbS-OA QDs into a PCPDTBT:PCBM blend, there is a decrease in the relative weight of the CT recombination lifetime (longer decay component); suggesting that there is an increase in the local dielectric constant of the ternary blends which affects the CT formation.

2.2 Experimental

2.2.1 Materials

PCPDTBT (M_W=38,000; PDI=2.3) (99.9%+) and $PC_{61}BM$ (99.9%+) were purchased from 1-material Inc. and Solenne B.V. respectively (see figure 1 for structures). Anhydrous Chlorobenzene was obtained from Sigma-Aldrich. These materials were used as received without any further purification.

PbS-OA QDs were synthesized according to previously reported methods.[26,27] For the 2.9 nm PbS QDs a lead precursor solution consisting of 1.5 g $PbAc_2 \cdot 3H_2O$ in 47.5 mL ODE and 2.5 mL OA was vacuum dried for an hour at 120ºC in a three-neck reaction flask. Then atmosphere was switched to argon and temperature was subsequently changed to 85 ºC. After that, the heating mantle was removed and a sulphur precursor of 420 µL TMS_2S in 10 mL of dried ODE was quickly injected. Extra oleic acid (3 mL) was injected 1 minute later and the flask was cooled down to room temperature by ice bath.

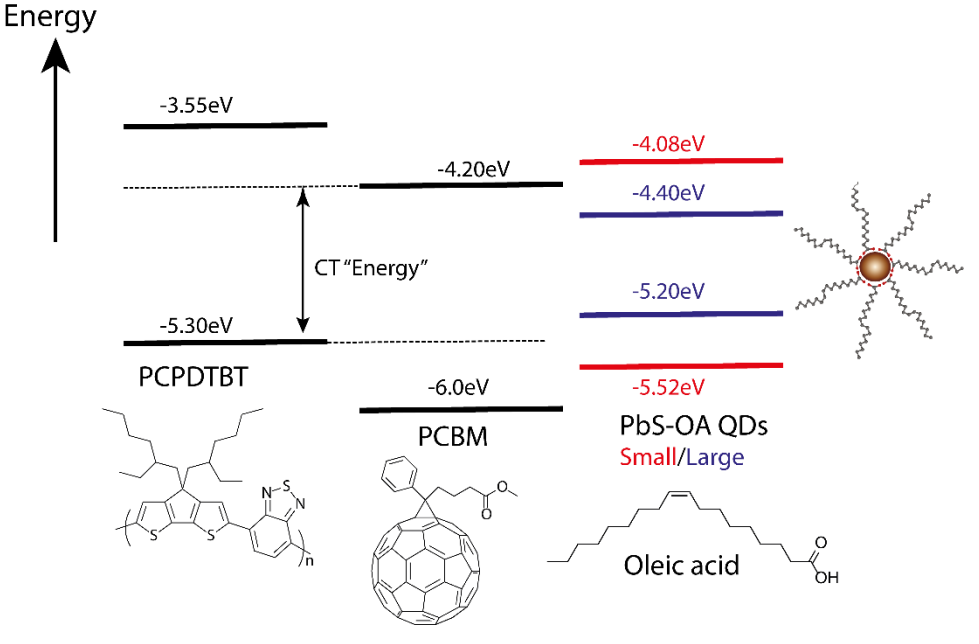

Figure 2.1: Chemical structures and energy levels of the materials used in this study: PCPDTBT: poly[2,6-(4,4-bis-(2-ethylhexyl)-4H-cyclopenta[2,1-b;3,4-b']dithiophene)-alt-4,7-(2,1,3-benzothiadiazole)]; PCBM: phenyl-C_{61}-butyric acid methyl ester and the organic capping ligand, oleic acid.

For the 5.8 nm PbS QDs, a lead precursor solution consisting of 0.75 g $PbAc_2 \cdot 3H_2O$ in 5 mL ODE and 15 mL OA was vacuum dried for an hour at 120 ºC in a three-neck reaction flask. The atmosphere was switched to argon and temperature was subsequently increased to 145 ºC. Then the heating mantle was removed and a sulphur precursor of 210 µL TMS_2S in 10 mL of dried ODE was quickly injected. After 3 minutes of growth the flask was cooled down to room temperature by ice bath. For both sizes of PbS QDs hexane and ethanol were added to the crude solution, followed by centrifugation to separate the QDs. Two more

washing steps were performed by re-dispersion in hexane and precipitation by ethanol. The final pellet was dissolved in anhydrous hexane and filtered through 450 μm PTFE filter. The QDs were later vacuum dried and re-dispersed in Chlorobenzene.

2.2.2 Film Preparation

1:1 (by weight) solutions of PCPDTBT and PCBM in Chlorobenzene (total concentration 20 mg/mL) were prepared to which either 0.25%, 0.5%, or 0.75% by weight of PbS-OA QDs were added to make ternary blends. Thin films of approximately 200nm were cast from warm solutions (60 ºC) using a blade coater on 1 cm^2 quartz substrates. The substrates were previously cleaned sequentially in soap, water, acetone and isopropanol, after which they were dried in an oven at 140 ºC to remove traces of solvent and then placed in a UV-Ozone oven for 20 minutes to increase surface wettability.

After deposition the samples were dried at 60 ºC for 5 minutes. Both deposition and storage were carried out in a Nitrogen filled glovebox.

2.2.3 UV-Vis Absorption Spectroscopy

Absorption measurements were carried out on (masked) areas of films on 1 cm^2 quartz substrates using a Shimadzu 3600 UV-VIS-NIR spectrophotometer. Where noted, absorption measurements of solutions were carried out in quartz cuvettes with 2 mm path length.

2.2.4 Photoluminescence Spectroscopy

Steady-state measurements were carried in out in a Nitrogen filled sample holder in transmission mode. The excitation source was the second harmonic (approximately 400 nm) of a mode-locked Ti:Sapphire laser (Mira 900, Coherent) delivering 150 ps pulses at a repetition rate of 76 MHz. The laser power was adjusted using neutral density filters; and the excitation beam was spatially limited by an iris. The beam was focused with a 150 mm focal length lens onto a spot of approximately 50 μm. Steady state spectra were collected by a spectrometer with a grating of 50 lines/mm and recorded with a inline diode array (ANDOR iDus) sensitive between 800 nm and 1.7 μm.

For time resolved measurements, the same pulsed excitation source was used. Spectra were collected on a Hamamatsu streak camera (Hamamatsu, Japan) working in Synchroscan mode (time resolution~2 ps) with a cathode sensitive in the infrared.

For measurement of the PbS-OA QD lifetime, a pulse-picker decreasing the laser repetition rate in conjunction with a slow-speed sweep unit of the streak camera (single-sweep mode) were used. All spectra were corrected for the spectral response of the instrument using a calibrated lamp.

2.3 Results and Discussion

Figure 2.1 shows the band alignment and structures of the materials we used in this study. HOMO and LUMO levels for PCPDTBT and PCBM have been taken from literature [25,28] and the electron affinity (EA) and ionization potential (IP) of the PbS QDs were estimated by a method previously employed by Gocalinska *et al* [29] based on the bandgap, EA, IP, and the effective masses of charge carriers in bulk PbS. The band gaps of the studied PbS-OA QDs were obtained from the position of the first excitonic absorption feature in the UV-Vis spectra. It should however be noted that the energy level positions may differ locally and that the EA and IP values of the QDs come mainly from theoretical considerations.

Figure 2.2(a) shows the absorption and photoluminescence spectra of pristine PCPCTBT and of a 1:1 PCPDTBT:PCBM blend. When the pristine polymer is mixed with PCBM the polymer photoluminescence is quenched; instead, emission from a new state at a lower energy (the CT state) is observed with a longer lifetime (~650 ps) compared to the pristine polymer luminescence lifetime (~180 ps) (Figure 2.2(b)). Previous work has established that the CT photoluminescence in PCPDTBT:PCBM blends is heavily influenced by the average dielectric constant of the blend, displaying a marked red-shift with the increase of the PCBM content.[24]

Scharber et al., have also shown that in the higher crystalline homologue of PCPDTBT, namely Si-PCPDTBT, the CT recombination can be supressed, and the resulting devices perform better.[30] This observation is further underscored by experiments using processing additives such as octanedithiol (ODT) in blends of PCPDTBT:PCBM, demonstrating suppression of CT recombination can also be achieved by altering the morphology of the BHJ, i.e. increasing the pristine D/A domain sizes. This is also followed by an increase in charge carrier mobilities and a decrease in bimolecular recombination and increase of the solar cell performance.[10]

These studies point to the fact that CT recombination depends not only on the dielectric constant but also on the crystallinity of the blend and its morphology, which can have important implications for the final performance in devices.

As we aim to study the variation of the CT emission as a function of amount of QDs, the main challenge lies in the fact that the photophysical properties of BHJ blends are also dependent on their (nano)morphology. This limitation is resolved in practice by using relatively low dilution levels; in our case, we have kept it at ≤0.75% by weight – thus aiming to study the effect of the *local* dielectric constant of the blend on the CT emission.

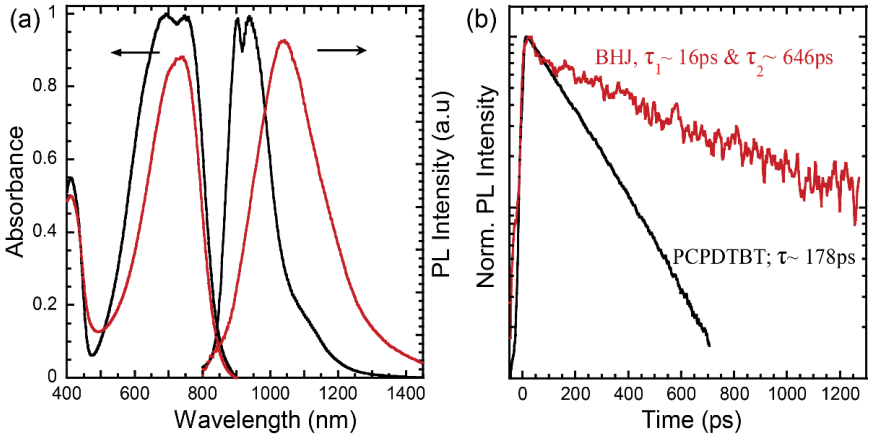

Figure 2.2: (a) Absorbance and PL spectra of pristine PCPDTBT (black lines) and a 1:1 PCPDTBT:PCBM blend (red lines), note that the emission of the CT state in the blend has been scaled up for convenience; (b) PL decay integrated over all spectra for PCPDTBT (black line) and a PCPDTBT:PCBM BHJ (red line) showing the long lived CT state PL compared to that of the pristine polymer.

Figure 2.3(a) shows the absorption and photoluminescence spectra of the first batch of PbS-OA QDs used in this study featuring an excitonic peak at 1530 nm (corresponding to average particle radius of ~5.8 nm). The relatively small stokes shift and symmetric peak shape is indicative of the good quality and small size polydispersity of the samples.[31] We chose this size of QDs because their photoluminescence is at a lower energy compared to the CT emission of the BHJ, making the analysis of the data simpler. The photoluminescence spectra for ternary PCPDTBT:PCBM blends with either 0.25%, 0.50%, or 0.75% by weight of these PbS-OA QDs are shown in Figure 2.4(b). As mentioned earlier, we selected such

small weight percentages in order to minimize the effects of the QDs on the thin film morphology, to assess how their simple presence, i.e., their dielectric constant affects the CT photoluminescence.

The steady-state PL spectra shown in Figure 2.3(b) of these ternary blends exhibit two distinct peaks, belonging to the CT state (approximately 1100 nm) and to the PbS-OA QDs (approximately 1580 nm), respectively. However, there is no clear trend in the CT photoluminescence peak energy as a function of amount of added QDs. To gain further insight into the effect of the QD addition on the CT recombination, we carried out time-resolved photoluminescence measurements on the blends. CT photoluminescence decay curves are shown in Figure 2.3(c) and corresponding streak camera images are provided in Figure 2.4(a-d), the extracted CT photoluminescence lifetimes are also summarized in Table 2.1. At first we note a strong variation of the intensity of the CT recombination upon addition of the QDs. The rather weak decay can be modelled with a biexponential behaviour described by the function: $y(t) = Aexp(-t / \tau_1) + Bexp(-t / \tau_2)$; where τ_1 and τ_2 represent fast and slow decay components, respectively; with A and B as coefficients describing their relative weights.

In analysing the data, we fixed $\tau_2 = 650$ ps; as this is the typical lifetime for the CT recombination[32] as shown in Figure 2.3(b). We therefore followed the evolution of τ_1 with amount of additive. The relative decrease in CT PL intensity (overall CT emission in Figure 2.4) on addition of QDs indicates a decrease in the initial population of the CT state. The decrease of the population of the CT state and the corresponding increase in the singlet exciton population is also confirmed by the decrease of the weight of the CT component (B coefficient) of the decay dynamics, see Figure 2.4(c) and Table 2.1. It is important to note that the decay traces are extracted in the low energy tail of the emission (between 950 and 1050 nm) explaining the very weak and noisy signal.

QD Size	Binary	Ternary (0.25wt%)	Ternary (0.50wt%)	Ternary (0.75wt%)
Large	66.2 (29%)	56.1 (42%)	27.8 (76%)	15.1 (82%)
Small	68.9 (33%)	22.2 (62%)	26.4 (56%)	26.6 (60%)

Table 2.1: Summary of the extracted lifetimes (in picoseconds) and corresponding weights for the ternary blends for QDs in Figures 2.4 and 2.5; (note that τ_2 was fixed to 650 ps). Values in brackets represent relative contributions calculated by $A/(A+B)$ expressed as a percentage.

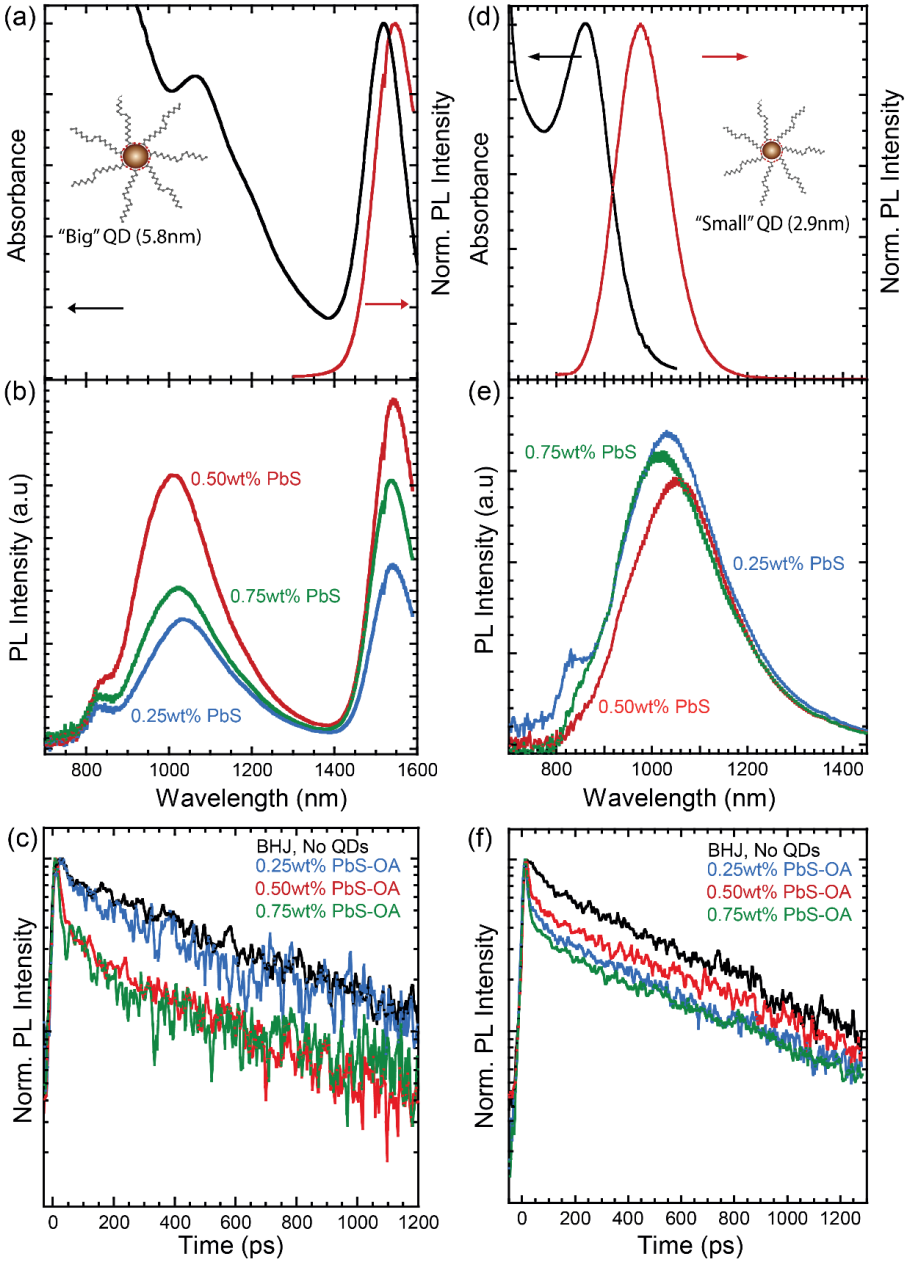

Figure 2.3: Normalized Absorbance (black line) and PL spectra (red line) of the large PbS-OA QDs in Chlorobenzene; (b) PL spectra of representative ternary blends with different %wts of large PbS-OA QDs (c) PL decay curves for the same blends in (b); the fast component becomes more prominent with increasing amounts of NCs in the blends (decay taken between 950nm - 1050nm); (d-f) are corresponding measurements with smaller QDs

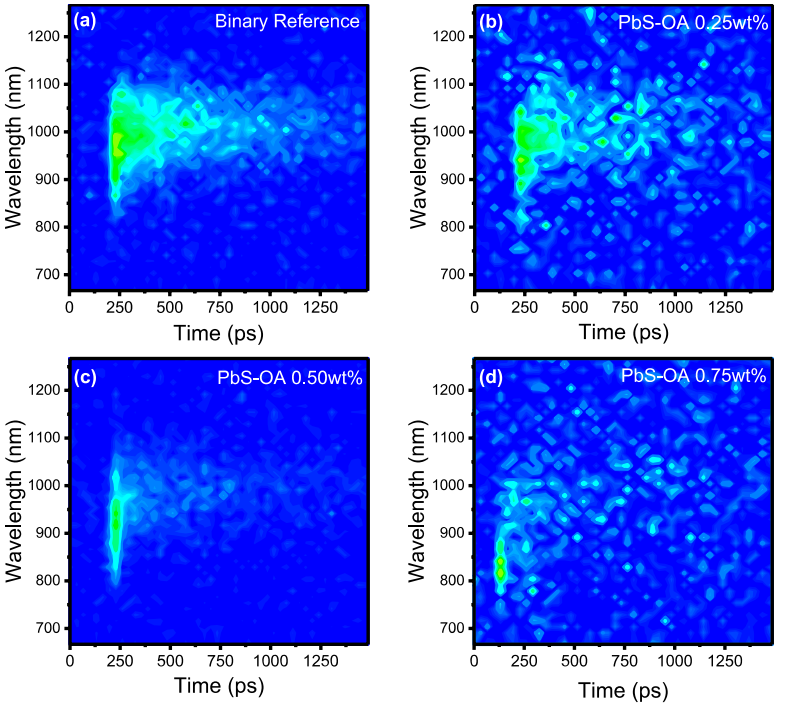

Figure 2.4: (a-d) Representative false colour streak camera images for the ternary blends made with the larger QDs (excitonic peak at 1530 nm).

To ascertain that the decrease in the CT state PL lifetime is due to a local dielectric effect, and not to energy transfer to the PbS QDs, we repeated the same experiment with the smaller batch of PbS-OA QDs, this time with excitonic peak at ~855 nm (i.e. with QDs having a bandgap larger than the CT state energy, and size ~2.9 nm). The absorbance and PL spectra of this batch of QDs are shown in Figure 2.3(d). Obviously, the steady state PL spectra of films made with these smaller QDs show a marked difference from the previous spectra due to the fact that the PbS-OA PL overlaps with the CT state emission, resulting in a single broad peak centred around 1150 nm as can be seen in Figure 2.3(e).

Time-resolved measurements on the ternary blends with small QDs are shown in Figure 2.3(f) and their lifetimes are summarized in Table 2.1. In the decay traces there is no evidence of the longer lifetime expected from the QDs. The QDs used have been measured in a matrix of PMMA, where they display a decay time of about 1 μs (see Figure 2.6). In the ternary blend because of their very low concentration and the very long decay time it is impossible to detect the decay. Although, in this

case (see streak images in Figure 2.5(a-d)) the decrease of intensity of the CT state emission seems less evident than in the previous set of samples; we observe a similar trend of the lifetimes – with a decrease of τ_1 and an increase of its relative weight when QDs are added, once again keeping τ_2 fixed at 650 ps in the fitting process.

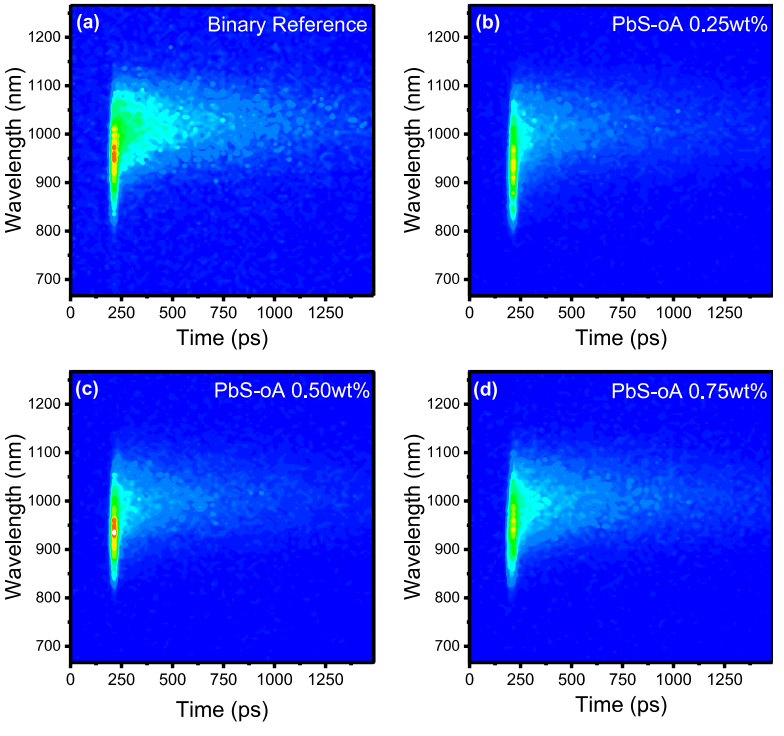

Figure 2.4: (a-d) Representative false colour streak camera images for the ternary blends made with the smaller QDs (excitonic peak at 950nm).

The identical features of the measurements obtained with different size of QDs excludes electron, hole or energy transfer as a cause of interaction between the CT states and the QDs, and seems to confirm that the interaction between the QDs and the CT emission is probably through the dielectric constant. Previous work by Kahmann *et al* on blends of PCPDTBT and PbS-OA QDs has established that the long oleic acid capping ligands largely supresses the possibility of charge transfer between the QDs and the surrounding organic matrix[28]; this, together with the very small amounts of PbS-OA QDs used lead us to conclude that there is no significant charge transfer between the polymer:fullerene system and the PbS-OA QDs.

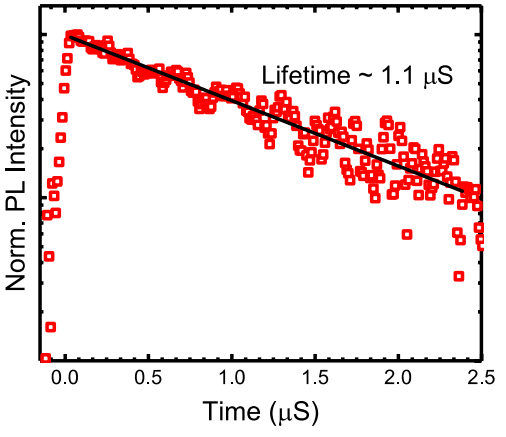

Figure 2.6: Time resolved PL for a thin film of the small QDs in a PMMA matrix.

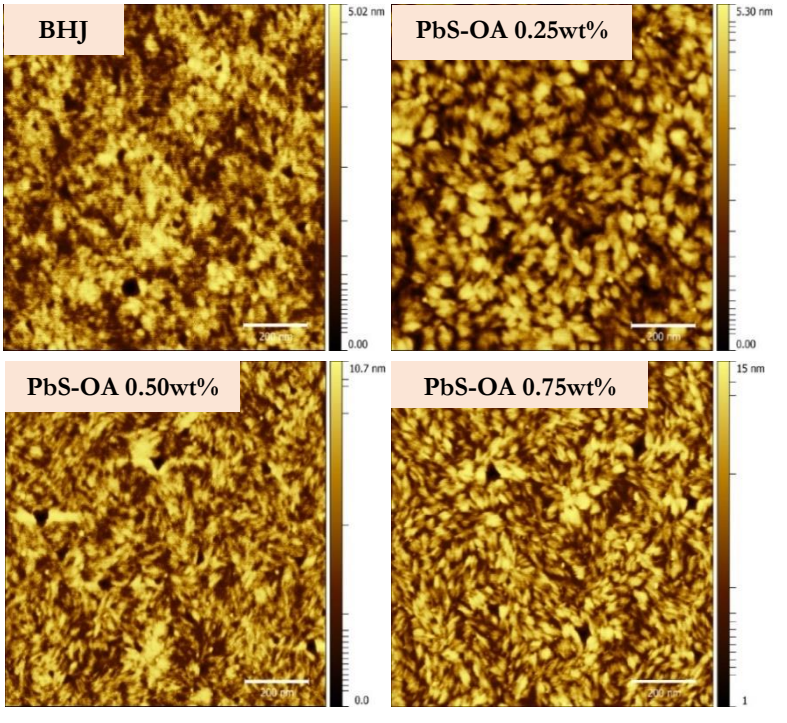

Figure 2.7: Representative atomic force microscope images of the topology of the ternary blends (with small NCs); all samples have root-mean-square roughness on the order of 0.35 to 0.7 nm. Scale bars represent 200 nm lengths

Unfortunately, the sensitivity observed for the CT state to the local morphology of the BHJ[19] makes it very difficult to make samples with higher amount of QDs, which would clearly demonstrate their effect on the dielectric constant; without altering the blend morphology. Atomic Force Microscopy (AFM) measurements on both samples with and without the NC additives show no significant difference in terms of surface roughness (less than 1 nm) and only very little morphological differences appear with the highest QD content (see Figure 2.7). It is important to note that due to our use of weight-percentages, we have approximately 70 times more small particles than large ones in the corresponding samples.

2.4 Conclusion

In conclusion, we studied the effect of a high-ε_r additive: oleic acid capped PbS QDs, on the CT emission of a BHJ composed of PCPDTBT and PCBM. Our results with QDs of different sizes indicate that even at low dilution levels (0.25% - 0.75% by weight), there is a decrease of the initially generated CT population. We explain these findings as being due to an increase in the local dielectric constant of the ternary blends. Our results suggest that using QDs as an additive can be a feasible approach to increase the local ε_r of BHJ blends.

References

[1] J. Zhao, Y. Li, G. Yang, K. Jiang, H. Lin, H. Ade, W. Ma, H. Yan, *Nat. Energy* **2016**, *1*, 15027.

[2] G. Luo, X. Ren, S. Zhang, H. Wu, W. C. H. Choy, Z. He, Y. Cao, *Small* **2016**, *12*, 1547.

[3] S. Zhang, L. Ye, J. Hou, *Adv. Energy Mater.* **2016**, *6*, 1502529.

[4] J. Van Der Horst, P. A. Bobbert, M. A. J. Michels, H. Bässler, J. Van Der Horst, P. A. Bobbert, M. A. J. Michels, **2013**, *6950*, DOI 10.1063/1.1356015.

[5] L. J. A. Koster, S. E. Shaheen, J. C. Hummelen, *Adv. Energy Mater.* **2012**, *2*, 1246.

[6] S. Chen, S. W. Tsang, T. H. Lai, J. R. Reynolds, F. So, *Adv. Mater.* **2014**, *26*, 6125.

[7] M. Manca, C. Piliego, E. Wang, M. R. Andersson, A. Mura, M. a. Loi, *J. Mater. Chem. A* **2013**, *1*, 7321.

[8] D. Veldman, O. Ipek, S. C. J. Meskers, J. Sweelssen, M. M. Koetse, S. C. Veenstra, J. M. Kroon, S. S. van Bavel, J. Loos, R. A. J. Janssen, *J. Am. Chem. Soc.* **2008**, *130*, 7721.

[9] C. Piliego, M. A. Loi, *J. Mater. Chem.* **2012**, *22*, 4141.

[10] M. C. Scharber, C. Lungenschmied, H.-J. Egelhaaf, G. Matt, M. Bednorz, T. Fromherz, J. Gao, D. Jarzab, M. a. Loi, *Energy Environ. Sci.* **2011**, *4*, 5077.

[11] N. Camaioni, R. Po, *J. Phys. Chem. Lett.* **2013**, DOI dx.doi.org/10.1021/jz400374p.

[12] H. J. Son, B. Carsten, I. H. Jung, L. Yu, *Energy Environ. Sci.* **2012**, *5*, 8158.

[13] S. Torabi, F. Jahani, I. Van Severen, C. Kanimozhi, S. Patil, R. W. A. Havenith, R. C. Chiechi, L. Lutsen, D. J. M. Vanderzande, T. J. Cleij, J. C. Hummelen, L. J. A. Koster, *Adv. Funct. Mater.* **2015**, *25*, 150.

[14] M. Breselge, I. Van Severen, L. Lutsen, P. Adriaensens, J. Manca, D. Vanderzande, T. Cleij, *Thin Solid Films* **2006**, *511–512*, 328.

[15] N. Cho, C. W. Schlenker, K. M. Knesting, P. Koelsch, H. L. Yip, D. S. Ginger, A. K. Y. Jen, *Adv. Energy Mater.* **2014**, *4*, 1301857.

[16] X. Chen, Z. Zhang, Z. Ding, J. Liu, L. Wang, *Angew. Chemie - Int. Ed.* **2016**, *55*, 10376.

[17] F. Jahani, S. Torabi, R. C. Chiechi, L. J. A. Koster, J. C. Hummelen, L. Jan, A. Koster, J. C. Hummelen, *Chem. Commun.* **2014**, *50*, 10645.

[18] S. Zhang, Z. Zhang, J. Liu, L. Wang, *Adv. Funct. Mater.* **2016**, *26*, 6107.

[19] A. Dieckmann, H. Bässler, P. M. Borsenberger, *J. Chem Phys* **1993**, *99*, 8136.

[20] D. Hertel, H. Bässler, *ChemPhysChem* **2008**, *9*, 666.

[21] C. Brückner, C. Walter, M. Stolte, B. Braïda, K. Meerholz, F. Würthner, B. Engels, *J. Phys. Chem. C* **2015**, *119*, 17602.

[22] C. Poelking, M. Tietze, C. Elschner, S. Olthof, D. Hertel, B. Baumeier, F. Würthner, K. Meerholz, K. Leo, D. Andrienko, *Nat. Mater.* **2014**, *14*, 434.

[23] D. D. W. Grinolds, P. R. Brown, D. K. Harris, V. Bulovic, M. G. Bawendi, *Nano Lett.* **2015**, *15*, 21.

[24] D. Jarzab, F. Cordella, J. Gao, M. Scharber, H. J. Egelhaaf, M. A. Loi, *Adv. Energy Mater.* **2011**, *1*, 604.

[25] M. A. Loi, S. Toffanin, M. Muccini, M. Forster, U. Scherf, M. Scharber, *Adv. Funct. Mater.* **2007**, *17*, 2111.

[26] L. Lai, L. Protesescu, M. V Kovalenko, M. A. Loi, *Phys. Chem. Chem. Phys.* **2014**, *16*, 736.

[27] M. A. Hines, G. D. Scholes, *Adv. Mater.* **2003**, *15*, 1844.

[28] S. Kahmann, A. Mura, L. Protesescu, M. V. Kovalenko, C. J. Brabec, M. A. Loi, *J. Mater. Chem. C* **2015**, *3*, 5499.

[29] A. Gocalińska, M. Saba, F. Quochi, M. Marceddu, K. Szendrei, J. Gao, M. A. Loi, M. Yarema, R. Seyrkammer, W. Heiss, A. Mura, G. Bongiovanni, *J. Phys. Chem. Lett.* **2010**, *1*, 1149.

[30] M. C. Scharber, M. Koppe, J. Gao, F. Cordella, M. A. Loi, P. Denk, M. Morana, H. J. Egelhaaf, K. Forberich, G. Dennler, R. Gaudiana, D. Waller, Z. Zhu, X. Shi, C. J. Brabec, *Adv. Mater.* **2010**, *22*, 367.

[31] L. Cademartiri, J. Bertolotti, R. Sapienza, D. S. Wiersma, A. Georg von Freymann, Geoffrey A. Ozin, *J. Phys. Chem. B* **2006**, *110*, 671.

[32] C. Deibe, T. Strobe, V. Dyakonov, *Adv. Mater.* **2010**, *22*, 4097.